Sequential effects in two-choice reaction time tasks: decomposition and synthesis of mechanisms

Supplement to "Sequential Effects in Two-Choice Reaction Time Tasks: Decomposition and Synthesis of Mechanisms" by Juan Gao, KongFatt Wong-Lin, Philip Holmes, Patrick Simen, and Jonathan D. Cohen, *Neural Computation*, September 2009, Vol. 21, No. 9, pp. 2407–2436.

Sequential effects in two-choice reaction time tasks: Decomposition and synthesis of mechanisms. Supplementary Materials.

Juan Gao, KongFatt Wong-Lin, Philip Holmes, Patrick Simen and Jonathan D. Cohen

1 Decision dynamics and residual activity during RSI

This section provides additional evidence in support of the findings of Section 3.1.1 of the main text regarding the effects of residual activity, and for the simplified model of Eqn. (2) adopted in Section 2.1.2.

Since stimuli are absent during RSI, external inputs ρ_i to the decision units are set to zero and the noise-free dynamics of Eqn. (1) are described by

$$\tau_c \frac{dx_1}{dt} = -kx_1 - \frac{\beta}{1+e^{-G(x_2-d)}},$$
$$\tau_c \frac{dx_2}{dt} = -kx_2 - \frac{\beta}{1+e^{-G(x_1-d)}}.$$

This system is reflection-symmetric about the diagonal $x_1 = x_2$ and has a unique stable fixed point at $(x_1, x_2) = (\bar{x}, \bar{x})$, where

$$1 + e^{-G(\bar{x}-d)} = -\frac{\beta}{k\bar{x}}.$$

Assuming that the previous stimulus is 1, the phase portrait is shown in Supplementary Fig. 1 for the parameters specified in Section 2.1.1 of the main text. During the RSI the activity of unit 2 (the loser) is strongly depressed and overshoots before approaching $(x_1, x_2) \approx (-0.2, -0.2)$. This is because the winning unit's activity remains positive and close to threshold due to the low decay rate $k = 0.2$, while the inhibition term $-\beta/[1 + \exp(-G(x_1 - d))]$ provides a negative input current to unit 2.

Here a two-second RSI is used, but for every RSI in the range explored in Soetens et al. (1985) the state (x_1, x_2) lingers near the dip, leading to unreasonably long decision times (~ 700 ms) for alternations, and near zero for repetitions, as shown in Supplementary Fig. 2. Moreover, when biases

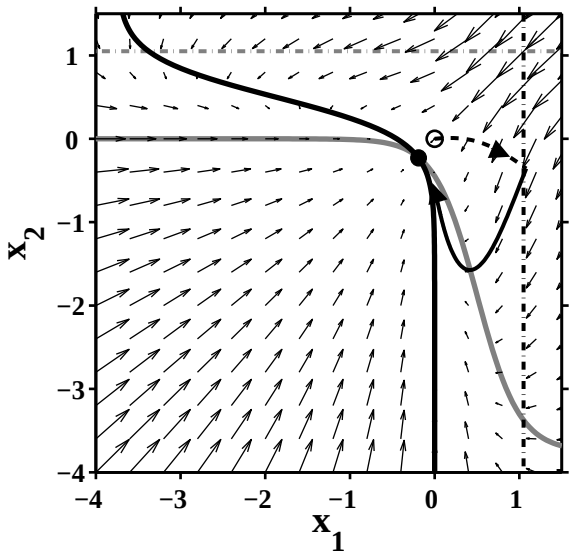

Figure 1: **Phase plane of the decision network.** Dashed black curve with arrow shows a noise-free trajectory of Eqn. 1 in main text with stimulus on, starting from open circle at stimulus presentation; solid black curve with arrow shows subsequent decay of activity and approach to fixed point $(\bar{x}_1, \bar{x}_2)$ (filled black circle) during a two-second RSI. Thick black (grey) curve: nullcline for x_1 (x_2). Vectorfields (thin arrows), and thresholds (dot-dashed lines) are also shown. Parameters are as specified in Section 2.1.1 of main text throughout trial and RSI.

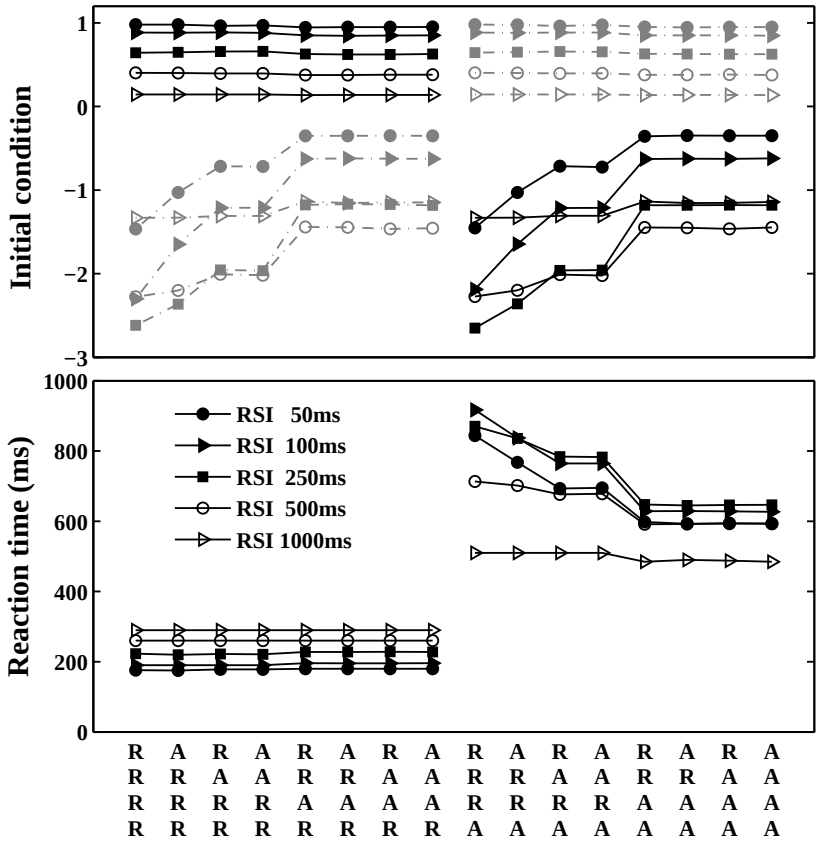

Figure 2: **Previous connectionist parameters produce long RTs.** Predicted residual activity using the parameters of Section 2.1.1 of main text throughout trial and RSI: RTs are much longer (overall mean $\approx$ 600ms) than those in experiments of Soetens et al. (1985). Format is as in Fig. 3 of main text, with initial conditions in top panel and resulting RTs below.

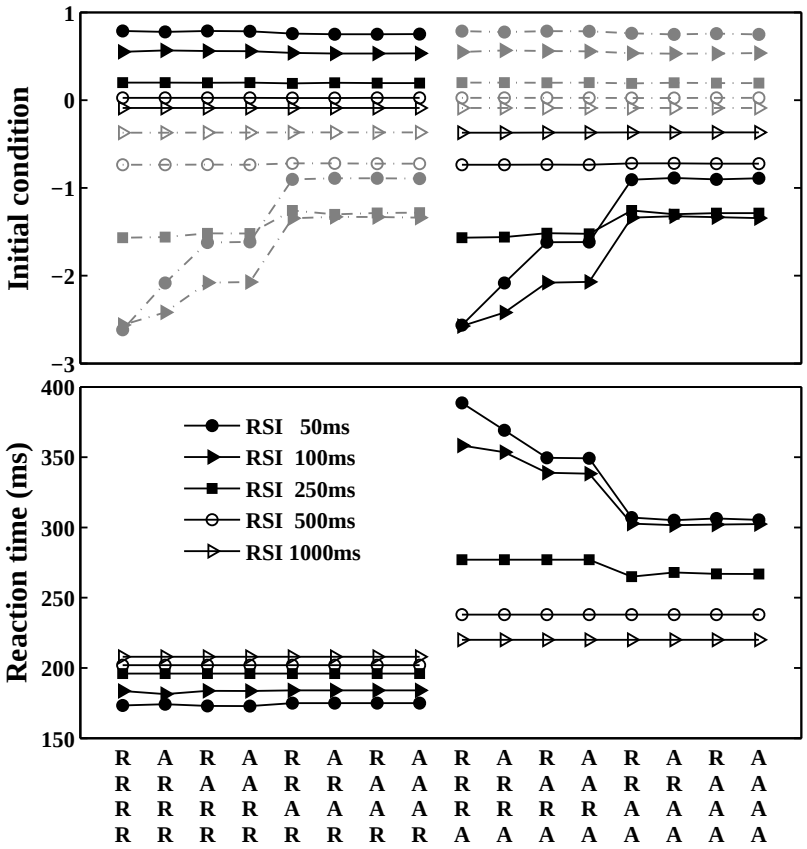

Figure 3: **Effects of time constant of decision units on residual decay and reaction times.** Predicted residual activity using $\tau_c = 0.03$ instead of $\tau_c = 0.1$ which increases decay rate, inhibition and input levels throughout trial and RSI. Format is as in Fig. 3 of main text and Supplementary Fig. 2.

from ACC and PFC, which can change the input currents, are included, it can happen that one decision unit is permanently suppressed and only the other crosses threshold, preventing responses to alternations altogether. Intuitively this suggests two possibilities: (1) The parameters of Usher and McClelland (2001) and Cho et al. (2002) are not applicable to the data of Soetens et al. (1985); (2) the parameters are reasonable when stimuli are present, but decay rates and/or inhibitory currents substantially increase during RSI.

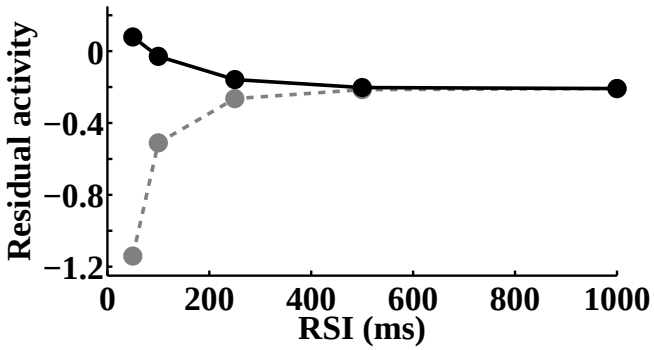

Figure 4: **Residual activities decay during RSI.** Residual activities of the winning (solid black) and losing (grey dashed) units in the last trial decay to a common baseline as RSI increases, reaching equilibrium by ≈ 0.5s. Also see Supplementary Fig. 1.

To test these two possibilities, we considered: (1) smaller values of τ_c, which effectively increase the decay, inhibition and external input currents during trial and RSI; and (2) larger values of decay rate and inhibition during RSI only. Specifically we set $\tau_c = 0.03$ (in place of 0.1) in the former case and $k = 4, \beta = 15$ (in place of 0.2 and 0.75) in the latter, leaving the position of the stable fixed point unchanged. These modifications respectively produce the RTs shown in Supplementary Fig. 3 and in Fig. 3 of the main text, confirming that residual activity alone cannot lead to higher order AF. Further exploration shows that, for $k > 4$, residual activity causes pure first-order facilitation for RSIs throughout the range $50 - 1000$ ms, so that earlier trials in the sequence do not influence residual activity.

In Supplementary Fig. 4 we plot the residual activities of the two units *vs* RSI values using $k = 4, \beta = 15$ to show that they can be reasonably approximated by exponential functions, supporting the simplified description

of residual activity of Eqn. (2) in Section 2.1.2 of the main text. In our formulation residual activities $x_j(t)$ can become negative, but they should not be literally interpreted as (non-negative) firing rates of neurons. In connectionist modeling the logistic function $f(x) > 0$ describes neuronal firing rate in place of x; here we use the latter to characterize neural activity, since f is a monotonic function of x.

2 Neural evidence of subjective expectancy

Fig. 5 shows neural activity which may reflect expectation-related activity. The bottom row shows the P300 amplitude in Sommer et al. (1999) while the top row shows the strength of expectation in the model . It can be observed that when RSI is very short (40 ms), there is relatively low P300 activity compared to longer RSI (500 ms), especiall at the flanks. In our modeling of the expectation-bias mechanism, we incorporate this experimental finding by having the expectation biasing strength to increase from zero, at a RSI below 40 ms and grows as RSI increases (section 2.1.3, main text).

3 Dynamics of conflict-based biasing strength in RSI

This section provides evidence in support of the strategic priming model developed in Section 2.1.4 of the main text.

Direct calculations using $E_n = \int_{trial} f(x_1(t))\, f(x_2(t))\, dt$ and $C_n = \lambda C_{n-1} + (1-\lambda)\alpha E_{n-1}$ with parameters specified in §2.1.1 of the main text and Botvinick et al. (2001), Jones et al. (2002) ($\alpha = -0.05$, $\lambda = 0.75$) reveal the strategic priming patterns shown in Supplementary Fig. 6. Priming strengths decrease as RSIs increase because neural activities have more time to decay for longer RSIs, producing lower conflict levels. In the bottom left panel, we plot the strategic priming strengths *vs* RSI and find almost perfect exponential decay during RSI. Further tests show that the timescale of this decay depends on strategic priming strength in an approximately linear manner (bottom right). This motivated the simplification of the conflict-based mechanism described in Eqns. (12-14) of the main text.

Note that the outlier in the bottom right panel represents the sequence RRA. The jumps up in priming strength (top panel) from AAR (the final

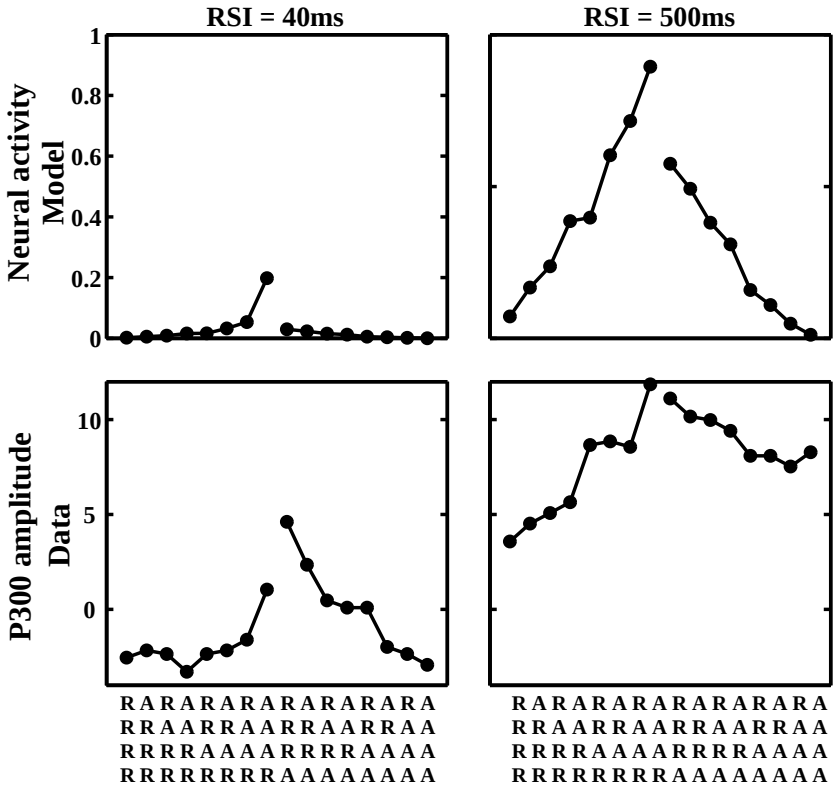

Figure 5: **Increase in expectation-related neural activity with increasing RSI.** Top: expectation-related neural activity predicted by the model for short (40ms, left) and long (500ms, right) RSIs. Values normalized to 1 for arbitrarily long sequences of A's followed by R. Bottom: P300 activity measured in experiment 2 in Sommer et al. (1999) (arbitrary units); data presented with author's permission. Labels on abscissa denote alternation (A) and repetition (R) sequences, reading from top to bottom.

sequence among RRR, ARR, RAR and AAR in which the last trial is a repetition) to RRA (the first sequence among RRA, ARA, RAA, AAA in which the last trial is an alternation) are introduced by the definition of C_n. Because no parameter used in this simulation is fitted, we ignore this detail and seek an approximation that captures the overall pattern of the dynamics.

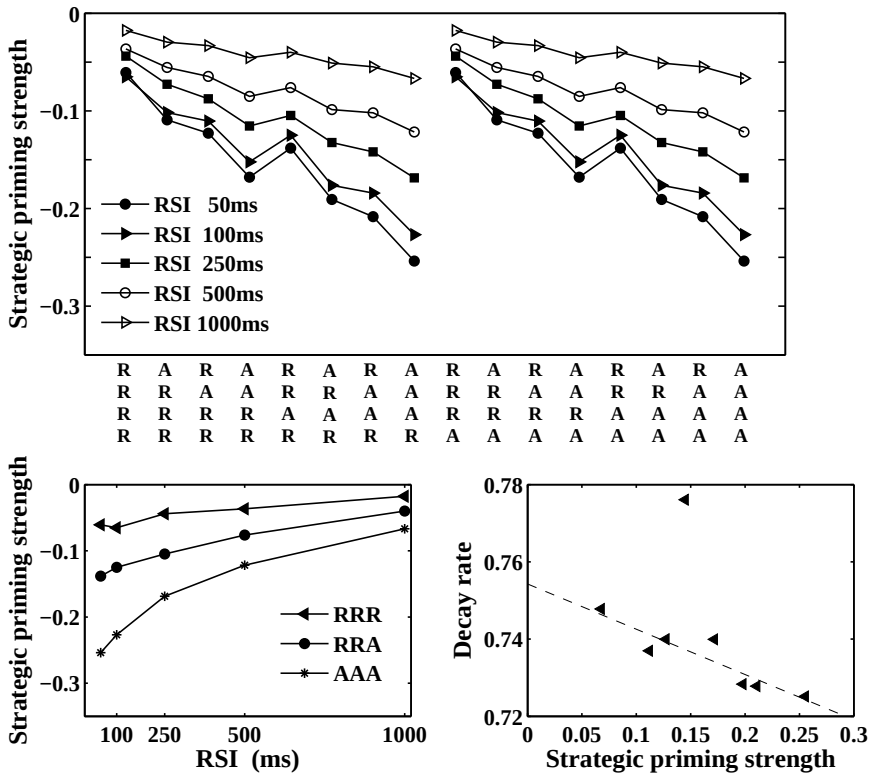

Figure 6: **Characteristics of conflict-induced biasing with different sequence histories and RSIs.** Top: strategic priming strength at beginning of current trial predicted by Eqns. (10-11) in main text, following different prior sequences shown on abcissa, with last trial at bottom. Bottom left: decay of strategic priming strength during RSI for three example sequences. Bottom right: fitted decay rate *vs* priming strength.

References

Botvinick, M., Braver, T., Barch, D., Carter, C., and Cohen, J. (2001). Conflict monitoring and cognitive control. *Psychological Review*, 108:624–652.

Cho, R., Nystrom, L., Brown, E., Jones, A., Braver, T., Holmes, P., and Cohen, J. (2002). Mechanisms underlying dependencies of performance on stimulus history in a two-alternative forced-choice task. *Cognitive, Affective and Behavioral Neuroscience*, 2:283–299.

Jones, A., Cho, R., Nystrom, L., Cohen, J., and Braver, T. (2002). A computational model of anterior cingulate function in speeded response tasks: Effects of frequency, sequence, and conflict. *Cognitive, Affective and Behavioral Neuroscience*, 2:300–317.

Soetens, E., Boer, L., and Hueting, J. (1985). Expectancy or automatic facilitation? Separating sequential effects in two-choice reaction time. *Journal of Experimental Psychology: Human Perception and Performance*, 11:598–616.

Sommer, W., Leuthold, H., and Soetens, E. (1999). Covert signs of expectancy in serial reaction time tasks revealed by event-related potentials. *Perception and Psychophysics*, 61:342–353.

Usher, M. and McClelland, J. (2001). The time course of perceptual choice: The leaky, competing accumulator model. *Psychological Review*, 108:550–592.